IEEE Photonics Journal
An IEEE Photonics Society Publication

Open Access

Nanoscale Noncoplanar Beam Splitters With Tunable Split Ratio

Volume 12, Number 2, April 2020

Shengnan Tian
Hanming Guo
Jinbing Hu
Songlin Zhuang

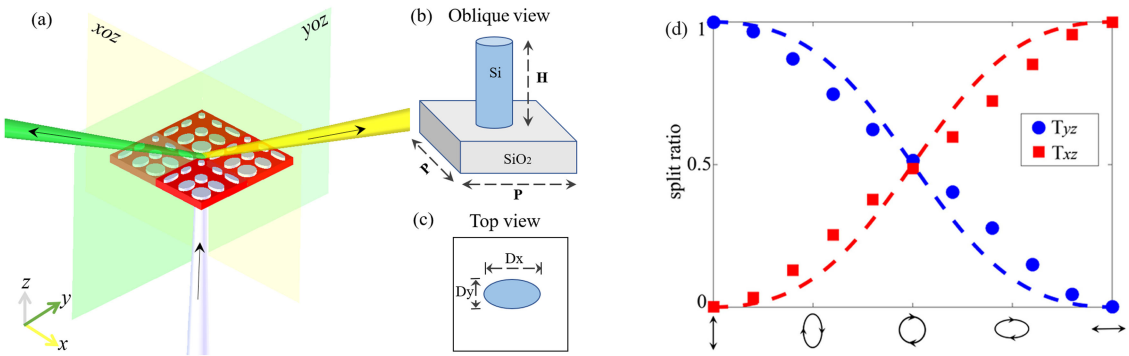

DOI: 10.1109/JPHOT.2020.2971113

Nanoscale Noncoplanar Beam Splitters With Tunable Split Ratio

Shengnan Tian, Hanming Guo, Jinbing Hu, and Songlin Zhuang

Engineering Research Center of Optical Instrument and System, Ministry of Education, Shanghai Key Lab of Modern Optical System, School of Optical-Electrical and Computer Engineering, University of Shanghai for Science and Technology, Shanghai 200093, China

DOI:10.1109/JPHOT.2020.2971113

Manuscript received October 28, 2019; revised January 9, 2020; accepted January 29, 2020. Date of publication February 2, 2020; date of current version March 9, 2020. This work was supported in part by the National Natural Science Foundation of China under Grant 61975125, in part by the National Natural Science Foundation of China under Grant 61805141, and in part by the Leading Academic Discipline Project of Shanghai Municipal Government under Grant S30502. Corresponding author: Jinbing Hu (e-mail: hujinbing@usst.edu.cn).

Abstract: Beam splitters, especially those with tunable split ratios, play significant role in interferometers, spectrometers, and communication systems. To this end, we proposed a polarization-controllable beam splitter based on dielectric metasurface composed of an array of dielectric pillars. The dielectric metasurface presents phase gradients along two orthogonal directions, say, *x*- and *y*-axis, with each phase gradient applicable to one of two orthogonal linear polarizations. Due to the orthogonality of the dual phase gradients in both position and polarization, an elliptically polarized incident beam can be diffracted into two refracted beams, one lies within *xoz* plane and the other in *yoz* plane. More importantly, the split ratio of the two refracted beams is continuously tunable by changing the ellipticity of incident beam. Under extreme case, *x*- or *y*-polarized incident beam is refracted into one beam, but in different planes for different kind of linear polarization. Besides, the refracted angle of each refracted beam in respective refracted plane can be easily set by adjusting the phase difference of adjacent rows or columns of metasurface. With same method, a polarization-controllable dual-wavelength beam splitter is also achieved on the basis of phase-gradient metasurface. Such a noncoplanar beam splitter with tunable split ratios may play significant role in novel miniature optical devices and systems.

Index Terms: Phase shift, metasurface, nanoantenna, beam splitters.

1. Introduction

A beam splitter is an essential component in various optical and photonic applications for separating lights with different polarizations, wavelengths, and powers [1]–[5]. Traditional beam splitters based on waveguides [6]–[8], gratings [9]–[11] and polymer platforms [12] are bulky and heavy, which limit their applications in compact and cost-effective systems. Metamaterials (MMs) are smartly engineered structures with rationally designed, nanostructured building blocks that allow us to no longer be constrained by the electromagnetic response of natural materials and their chemical compounds. Instead, we can tailor the shape and size of the structural units of a MM, tune the composition and morphology of the nanostructure, and achieve new, desired functionalities [13]. For example, by positioning metamaterials above a thick silver film separated by a silica dielectric spacer layer, or by suspending the metamaterials to reduce the effect of the substrate [14]–[16], enhancing and modifying the magnetic plasmon resonance in metamaterials can be

realized, which may find great potential applications in label-free biomedical sensing. Metasurfaces, comprising of a class of optical MMs with a reduced dimensionality, enable unprecedented control of the wavefront of light beam and thus have successfully opened a versatile avenue for the development of focusing and imaging devices, angular-momentum-based quantum information processing and integrated nano-optoelectronics [17]–[21]. At first, metasurfaces are designed using metals [22]–[24]. However, plasmonic metasurfaces suffer from high optical losses, especially at wavelengths shorter than the mid-IR. Although the reflection-type design can reduce the loss to some extent, the intrinsic heat dissipation is still a stumbling block to high efficiency of the plasmonic metasurface. This limitation can be overcome by replacing metals with all-dielectric structures [25], [26].

Actually, in addition to high efficiency, the split ratio is also an essential aspect to criticize the performance of metasurface-based beam splitter. If the split ratio of beam splitters can be flexibly modulated at will, then it will broaden the usage of beam splitters in various applications such as interferometers, spectrometers, and so on [27], [28]. Although some works have been reported on beam splitters with adjusting splitting ratios [29], [30], there are still some drawbacks in the implementation. For instance, the terahertz beam splitter designed by Wei *et al*. [29] was based on a metasurface with symmetric element arrangement and each of the two halves presents different phase gradient. The split ratio is tuned by shifting the relative position between the center of incident beam and the center of the metasurface. This kind of beam splitter may not be applicable to miniaturized optical instruments and systems where all devices are spatially unmovable. The beam splitter designed by Zhang *et al*. [30] is composed of two rows of cylinder arrays with two opposite phase gradients and its split ratio is adjusted by selectively increasing the losses of one of the rows of cylinders. Inevitably, the transmission efficiency gradually decreases as the increase of material loss.

Here, we numerically demonstrated polarization-controllable high-efficiency beam splitters based on phase-gradient metasurface. The beam splitter can refract a single incident beam into two refracted beams with arbitrary splitting ratios lying in two orthogonal planes. In the design, we first propose a metasurface which exhibits phase gradients along two orthogonal directions, say, *x*- and *y*-axis, thus named as dual phase-gradient metasurface. The proposed dual phase-gradient metasurface comprises an array of supercell array, each of which consists of $M \times N$ elliptical pillars. By properly choosing the lengths of major and minor axes of the elliptical pillars, phase shifts covering the range from 0 to 2π in two orthogonal directions can be obtained. On the basis of the dual phase-gradient metasurface, a noncoplanar beam splitter is designed. To demonstrate the splitting performance of the noncoplanar beam splitter, some numerical simulations are performed using commercial FDTD Solutions. The results show that the carefully designed noncoplanar beam splitter can refract a single normally-incident light beam into two cross polarized refracted beams, which lie in two orthogonal refracted planes. Particularly, when *x* or *y* linearly polarized beam is incident on the metasurface, the designed beam splitter function as double deflectors, with the deflected beam located in *xoz* plane or *yoz* plane, respectively. More importantly, unlike shifting the location of the metasurface [29] or increasing the losses level of cylinders [30], the split ratio between the two refracted beams of the proposed beam splitter can be tuned flexibly and continuously by manipulating the ellipticity of incident beam. Besides, the refracted angle of each refracted beam in respective refracted plane can be easily set independently by changing the size of the supercell. Furthermore, since the supercell can be designed at a specific wavelength, the noncoplanar beam splitter can also be designed as a polarization-controllable dual-wavelength beam splitter. We envision that this type of noncoplanar beam splitters with tunable split ratios have significant applications in complex miniaturized optical devices and systems.

2. Theoretical Analyses

Each unit cell of the metasurface can be optically taken as a waveguide truncated on both sides [31]. For unit cell with asymmetric cross-section, such as elliptical pillars, different lengths in major and minor axes exhibit different effective refractive indices, leading to different phases shifts. So,

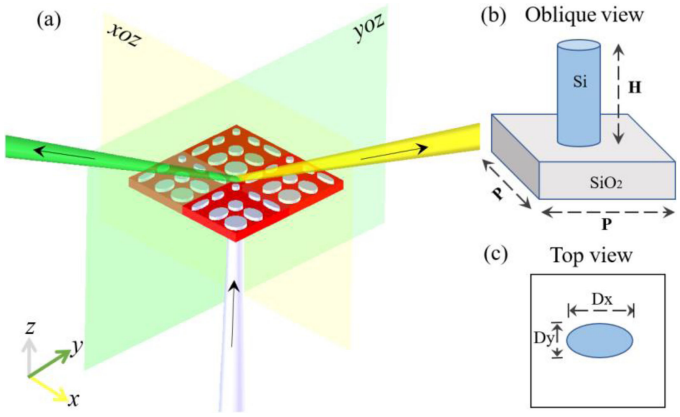

Fig. 1. Schematic of the noncoplanar beam splitter and its building block, the silicon elliptical pillar. (a). The beam splitter based on dual phase-gradient metasurface refracts a single normally-incident beam into two beams, which lie in two orthogonal refracted planes. (b and c) Oblique view and top view of the beam splitters building block formed by a silicon elliptical pillar sitting on a silica substrate with the side length P = 400 nm. The elliptical pillars have a fixed height of H = 715 nm and, by properly choosing their lengths along two orthogonal directions, D_x and D_y, the building blocks impose different phase shifts ϕ_x and ϕ_y.

by controlling the cross-section of elliptical pillars, phase shifts covering the range from 0 to 2π can be obtained, which is essential for the design of metasurface-based devices. For an elliptical pillar with no rotation, the major and minor axes can impose two polarization-dependent phase shifts on the wavefront of incident light. The transmission property of such nanostructure can be expressed using the Jones matrix

$$T = \begin{bmatrix} e^{i\phi_x} & 0 \\ 0 & e^{i\phi_y} \end{bmatrix}, \tag{1}$$

where ϕ_x, ϕ_y are phase shifts for *x*- and *y*-polarization, respectively. Different phase shifts ϕ_x, ϕ_y can be achieved by changing the cross-section of unit cell, that is, by changing the lengths of the major and minor axes of the elliptical pillar. In principle, it is attainable to design such an array of elliptical pillars whose phases ϕ_x remain unchanged while phases ϕ_y change periodically with the change of cross-section. Similarly, it is also fully realizable to design an array of elliptical pillars whose phases ϕ_y remain unchanged but phases ϕ_x change periodically with the change of cross-section. In other words, such birefringent nanostructures provide two degrees of freedom for phase control of incident light. Therefore, a metasurface with two independent gradients that correspond to *x*- and *y*-polarized incidence can be implemented. Since these two polarized incident beams are orthogonal, the phase gradients of the metasurface do not interfere with each other.

On the basis of above analysis, a dual phase-gradient metasurface composed of periodically arranged supercell arrays is proposed as schematically illustrated in Fig. 1(a). The supercell consists of $M \times N$ high refractive index silicon (n = 3.56) elliptical pillars with different cross-section, resting on an infinitely thick silica substrate as shown in Figs. 1(b) and (c). It has been demonstrated that high-ratio silicon nanopillars in the near infrared can independently and arbitrarily control phase and polarization of light beams with high transmittance at the subwavelength scale. Here, *P* denotes the side length of square unit cell, D_x and D_y denote the lengths of the major and minor axes of the elliptical pillars, respectively. To pattern two independent phase gradients with phase shifts covering from 0 to 2π on a single metasurface, the phases ϕ_x and ϕ_y of each unit cell must satisfy the condition described like this

$$\begin{cases} \phi_x(1, j) = \phi_x(2, j) = \cdots = \phi_x(M, j) \\ \phi_y(i, 1) = \phi_y(i, 2) = \cdots = \phi_y(i, N) \end{cases} \quad (i = 1, 2, \cdots M,\ j = 1, 2, \cdots N). \tag{2}$$

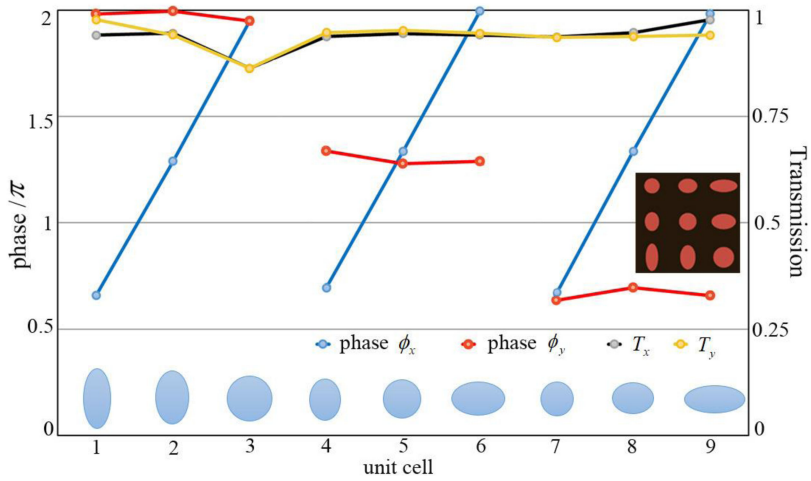

Fig. 2. The simulated propagation phases ϕ_x, ϕ_y and transmissions T_x, T_y of the designed elliptical pillars in a supercell. The pillars size (D_x and D_y) from 1 to 9 are $D_x = 140$, 172, 232, 160, 196, 272, 172, 212, 308 nm, and $D_y = 308$, 272, 232, 212, 192, 172, 168, 160, 140 nm. Insets: top view of the proposed supercell consisting of nine elliptical pillars.

Where i denotes row, and j denotes column. That is, phases ϕ_x and ϕ_y have incremental phase of $2\pi/M$ and $2\pi/N$ between adjacent rows and columns, respectively. It has been reported that due to the present of phase gradient along the interface, the refracted beam of metasurface is governed by the generalized Snell's law [32]. Following the same analysis, the metasurface with dual orthogonal phase gradients can control the propagation direction of refracted beam through the following expanded generalized Snell's law:

$$\sin(\theta_{t\zeta})n_{t\zeta} - \sin(\theta_i)n_i = \frac{\lambda}{2\pi}\frac{d\phi_\zeta}{d\zeta}, \qquad (\zeta = x, y) \tag{3}$$

where $d\phi_\zeta$ denotes the phase difference between adjacent unit cells along ζ axis. Equation (3) implies that the dual phase-gradient metasurface can refract incident beam into different planes at different refracted angles. In detail, when the metasurface is illuminated normally by x-polarized light, the refracted light will be located in xoz plane with refracted angle of θ_{tx}, and when the metasurface is illuminated normally by y-polarized light, the refracted light will be located in yoz plane with refracted angle of θ_{ty}. Furthermore, when the metasurface is illuminated normally by an elliptically polarized light, the metasurface will refract the incident light beam into two beams simultaneously, which are being within xoz plane and yoz plane, respectively.

Here, we set $N = M = 3$, other values of N, M could also be chosen. Hence, the incremental phase between adjacent rows (columns) is $2\pi/3$. To ensure high efficiency, elliptical pillar height H and the side length of square unit cell P (figures 1b, c) are optimized at the design wavelength of 915 nm. In this design, as each unit cell can be optically taken as a waveguide, the height of the unit cell should be tall enough to provide 2π phase coverage through a range of cross-sections, i.e., different lengths of major and minor axes of the elliptical pillar. Meanwhile, in order to deflect the incident light into the desired diffraction order, we set $P = 400$ nm and the elliptical pillar height $H = 715$ nm at the wavelength of 915 nm. We compute the transmissions T_x, T_y and phase shifts ϕ_x, ϕ_y of x- and y-polarized plane waves for all mutual values of the elliptical axes D_x and D_y in the range of $0.2P - 0.8P$ by using commercial FDTD Solutions (The simulated results are not shown here). Then, we select nine elliptical pillars that satisfy the phase condition in (2) to form the supercell. Fig. 2 shows the simulated results of the nine elliptical pillars, and the inset is the top view of the designed supercell. In Fig. 2, for the three elliptical pillars on the same row (as numbered for 1,2,3; 4,5,6; 7,8,9), their phases ϕ_x exhibit positive gradient ranging from 0 to 2π with an incremental phase of $2\pi/3$(as denoted by blue line), while phases ϕ_y remain unchanged

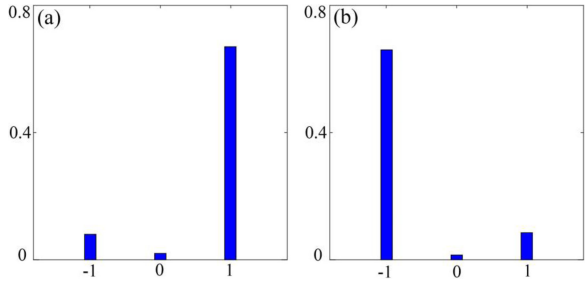

Fig. 3. The transmittance along different refracted angles θ by the designed beam splitter for (a) *x*-polarized incident light and (b) *y*-polarized incident light at the wavelength of 915 nm. The transmittance values are: (a) 0.08, 0.02, and 0.67 for -1, 0, and $+1$ diffraction orders in *xoz* plane, respectively; (b) 0.66, 0.015, and 0.085 for -1, 0, $+1$ diffraction orders in *yoz* plane.

(as denoted by red line). Similarly, for the three elliptical pillars on the same column (as numbered for 1,4,7; 2,5,8; 3,6,9), their phases ϕ_y exhibit negative gradient ranging from 0 to 2π with an incremental phase of $2\pi/3$(as denoted by red circles), while phases ϕ_x remain unchanged (as denoted by blue circles). In addition, as shown in the figure, the difference between the maximum and minimum transmittance is 0.11, and the maximum difference between the phase of elliptical pillar and the theoretical phase is 9.4 deg. These simulated results show the selected nine elliptical pillars have almost unity transmissions and required phases, which ensures the realization of dual phase-gradient metasurface.

3. Simulations and Discussions

On the basis of the supercell shown in Fig. 2, a noncoplanar beam splitter are elaborately designed and some numerical simulations are performed to verify the splitting properties of metasurface-based beam splitter using commercial FDTD Solutions, where an infinitely thick silica substrate, light beam with wavelength $\lambda = 915$ nm and periodic boundary conditions are utilized. In subsection 3.1, the refraction performance of the beam splitter is discussed in detail for normal incidence of linear polarization. Then, as an important aspect of a beam splitter, the adjustable split ratios are demonstrated in subsection 3.2 by changing the ellipticity of incident beam. In subsection 3.3, to display the freedom to set the refracted angles and select wavelengths along two orthogonal directions, another two noncoplanar beam splitters are designed and discussed.

3.1. Noncoplanar Beam Splitter With High-efficiency Splitting Performance

According to theoretical analysis, the incident beam will be refracted into different planes depending on its polarization. In particular, when the incident beam is *x*-polarized, the refracted beam will be located in *xoz* plane, and when the incident beam is *y*-polarized, the refracted beam will be located in *yoz* plane. Meanwhile, as the supercell has the periodicity of $P_x = NP = 1200$ nm with positive phase gradient along *x*-axis and $P_y = MP = 1200$ nm with negative phase gradient along *y*-axis, the beam splitter will refract *x*- and *y*-polarized incident beams into $+1$ and -1 diffraction order, respectively.

The refraction of the dual phase-gradient metasurface for *x*- and *y*-polarized incidence has been numerically simulated and the diffraction order distributions in *xoz* and *yoz* planes has been calculated. The simulated results are shown in Figs. 3(a) and 3(b), which shows that for normal incident beam of either *x*- or *y*-polarized, the dominant refracted beam is within one diffraction order. In detail, for *x*-polarized beam, the dominant refracted component appears at the angle of 49.69 deg and lies in *xoz* plane, corresponding to $+1$-order diffraction; for *y*-polarized beam, the dominant refracted component appears at the angle of -49.69 deg and lies in *yoz* plane, corresponding to -1-order diffraction. Theoretically, according to the parameters used in designing supercell the theoretical refracted angle given by (3) should be 49.69 deg and -49.69 deg, exactly

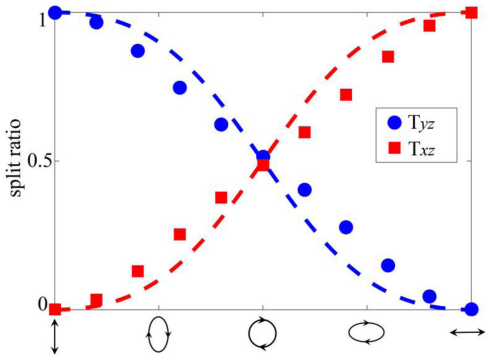

Fig. 4. The simulated performance of split ratios of the proposed noncoplanar beam splitter under the incident light with different ellipticity. The symbols, squares and dots, show the transmittance of two dominant refracted components in *xoz* and *yoz* planes. The dashed curves represent the theoretical results of the split ratios calculated by the normalized intensity of *x* component and *y* component of the E-field.

same as simulated value. The good consistency between the simulated results and the analytical results derived from (3) indicates the validity of the expanded generalized Snell's law in describing the split angles of the noncoplanar beam splitters. In addition, for x-polarized incident beam, the total transmittance is 0.77, in which the $+1$-order diffraction is 0.67, accounting for 87% of the total transmittance; for y-polarized incident beam, the total transmittance is 0.767, in which the $+1$-order diffraction is 0.66, accounting for 86% of the total transmittance. The loss is due to the fact that a small amount of energy is refracted to other diffraction orders, such as -1-order diffraction and $+1$-order diffraction for *x*- and *y*-polarized incident beam, respectively. The simulated results verify that the proposed beam splitter has good beam splitting performance and high efficiency.

3.2. Noncoplanar Beam Splitter With Tunable Split Ratios

Any elliptical polarization can be represented by two orthogonal linear polarizations, such as *x*- and *y*-polarizations. So, if the elliptical polarization of incident beam can be expressed as $[a, bi]^T$, then the values of a and b (represent *x*- and *y*-polarization components, respectively) determine the ellipticity of the incident beam. For example, when $a > b > 0$, the proportion of *x*-polarization is larger than *y*-polarization. Conversely, when $b > a > 0$, the proportion of *y*-polarized light is larger than *x*-polarization. In particular, the incident light is *x*-polarized light if $a \neq 0$, $b = 0$ and *y*-polarized light if $a = 0$, $b \neq 0$. For $a = b$, the proportion of *x*- and *y*-polarization is equal, so the incident light is circularly polarized light. Since the designed beam splitter is polarization-controllable, and the refracted beam in *xoz/yoz* plane is only related to the incidence of *x*-/*y*-polarized, arbitrary ratios between the two dominant refracted components of the transmitted light can be achieved flexibly by simply adjusting the ellipticity of the incident light.

The simulated performance of the proposed noncoplanar beam splitter under normally incident light with different ellipticity is shown in Fig. 4. Here, right handedness is chosen for elliptical polarization. Shown in Fig. 4, for *y*-polarized incidence, the transmittance of the dominant refracted component in *yoz* plane (labeled by T_{yz}) reaches a maximum value, which is almost equal to 1. However, at this time, the transmittance of the dominant refracted component in *xoz* plane (labeled by T_{xz}) is 0.001, which is completely negligible. As the *x*-polarization component increases, T_{xz} gradually increases while T_{yz} decreases. Particularly, when the incidence is circularly polarized, i.e., the proportion of *x*- and *y*-polarization is equal, the value of T_{xz} is nearly equal to T_{yz}. Beyond this, the proportion of *x*-polarization component exceeds *y*-polarization component, and correspondingly, the value of T_{xz} exceeds the value of T_{yz}. Finally, when the incidence is only *x*-polarized, the value of T_{xz} is maximized, and the value of T_{yz} is minimized. The ratio of the former to the latter is 0.999:0.001. The simulated results confirm that the split ratios of the noncoplanar beam splitter designed in this paper can be flexibly modulated by changing the ellipticity of incident beam.

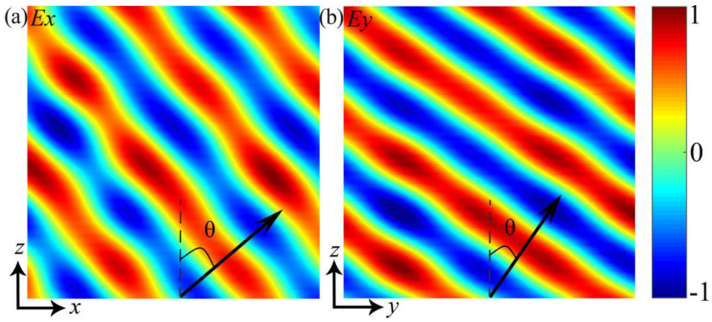

Fig. 5. The simulated normalized electric field distributions for the beam splitters with two different refracted angles. The transmitted E-field (a) E_x in *xoz* plane for *x*-polarized incident light and (b) E_y in *yoz* plane for *y*-polarized incident light at $\lambda = 915$ nm.

Compared with previously reported approaches of shifting the relative position between the center of incident beam and the center of the metasurface [25] and selectively increasing the losses of one of the rows of cylinders [26], the tunable strategy of ellipticity presented in this paper is more convenient, efficient, and universal in the fields of miniaturized optical devices and systems.

3.3. Noncoplanar Beam Splitter With Different Refracted Angles and Wavelengths

According to (3), the refracted angles θ_{tx} and θ_{ty} of the two refracted beams lying in *xoz* and *yoz* planes depend on the corresponding phase gradient $d\phi_x/dx$ and $d\phi_y/dy$ respectively. As the phase gradients of the two orthogonal directions of the metasurface designed herein are independent of each other, different phase gradients can be realized by changing the matrix orders of the supercell. Therefore, different refracted angles can be achieved by designing supercells of different orders.

Here, another supercell has been designed with size of 4×3 under the wavelength of 915 nm, i.e., the incremental phases $d\phi_x$, $d\phi_y$ of the dual phase-gradient metasurface are $2\pi/3$, $2\pi/4$, respectively. With the positive phase gradients in *x*- and *y*-axis, the beam splitter will refract *x*-polarized incidence into *xoz* plane and *y*-polarized incidence into *yoz* plane with $+1$-order diffraction, respectively. The simulated electric fields E_x and E_y in the transmission field of the beam splitter are shown in Figs. 5(a) and (b). As expected, the refracted component of the light for *x*-polarized incidence lies in *xoz* plane with a refracted angle of 49.69 deg, and similarly, the refracted component of the light for *y*-polarized incidence lies in *yoz* plane with a refracted angle of 34.88 deg. According to (3), the theoretical refracted angle for normal incidence can be calculated by $\theta = \sin^{-1}(\lambda/d)$, where d denotes the lattice length of the supercell. Here, the theoretical refracted angles θ_{tx} and θ_{ty} are 49.69 deg and 34.88 deg, exactly same as simulated value. Besides, the transmittance of the desired diffraction order for *x- (y-)* polarized incident light are obtained as 0.71 (0.76), accounting for 87% (89%) of the total transmittance.

Furthermore, according to theoretical analysis, the propagation phases ϕ_x and ϕ_y of each elliptical pillar can be independently tailored by changing the lengths of major and minor axes of the pillar. Meanwhile, since the major and minor axes of the pillar in the supercell are selected for a specific wavelength, the propagation phases ϕ_x and ϕ_y of each pillar are related to the wavelength of the incidence. Therefore, in theory, it is entirely possible to design an elliptical pillar whose propagation phase ϕ_x depends on λ_1, and the other phase ϕ_y depends on λ_2. In this way, a dual-wavelength beam splitter can be realized by using such elliptical pillars. To this end, a supercell has been designed with size of 4×3 for *x*-polarized incident light with wavelength of 460 nm and *y*-polarized incident light with wavelength of 530 nm. To reduce optical losses in visible region, elliptical cross section TiO_2 pillar sitting on a square silica substrate with side 200 nm long are selected, and all pillars have as same height as 600 nm. Similar to the aforementioned beam splitter in above subsection, the dominant refracted components are desired to be contained within $+1$-order diffraction in *xoz* and *yoz* planes when their corresponding polarization states of light

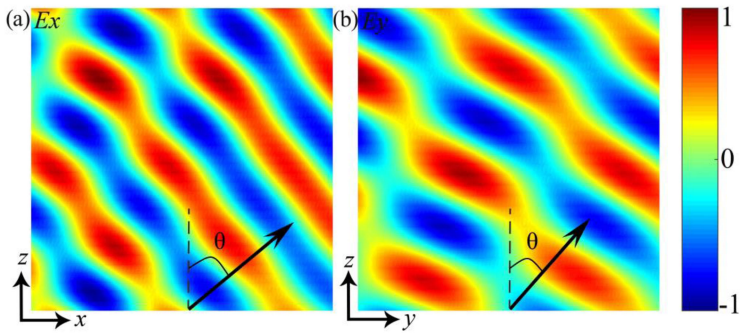

Fig. 6. The simulated normalized electric field distributions for noncoplanar beam splitters with two different wavelengths. The transmitted E-field (a) E_x in *xoz* plane for *x*-polarized incident light at $\lambda = 460$ nm and (b) E_y in *yoz* plane for *y*-polarized incident light at $\lambda = 530$ nm.

incident. The simulated electric fields E_x and E_y are plotted in Figs. 6(a) and (b), respectively. The simulated refracted angles θ_{tx} and θ_{ty} are 50.06 deg and 41.49 deg, respectively, which agree well with the theoretical values. The transmittance of the total diffraction orders and $+1$-order diffraction for *x*-polarized incident light also are calculated, they are 0.9 and 0.64, respectively. For *y*-polarized incident light, the corresponding transmittance are 0.9 and 0.56, respectively. Higher transmittance can be achieved by optimizing the geometric parameters of the supercell, such as the array orders, and the parameters of the elliptical pillars, such as the period, height, and the length of major and minor axes. Besides, all the refracted lights have well-fined wave-fronts, which verify that our proposed noncoplanar beam splitters have good splitting performance.

4. Conclusion

In conclusion, we propose a dual phase-gradient metasurface which exhibits phase gradients along two orthogonal directions. On the basis of the dual phase-gradient metasurface, we designed a noncoplanar beam splitter which can refract a single normally-incident light beam into one or two beams, depending on the polarization of incident beam. When the noncoplanar beam splitter is illuminated by *x- (y-)* polarized light, it can refract light into *xoz (yoz)* plane with high transmission efficiency. When the noncoplanar beam splitter is illuminated by elliptically polarized light, it can refract the light into two cross polarized beams, which lie in two orthogonal refracted planes. More importantly, the split ratios between the two dominant refracted components can be flexibly tuned by adjusting the ellipticity of the incident light which is more convenient, high-efficient, and universal in practical applications, instead of shifting the location of the metasurface or changing the losses level of the nanostructures reported in previous literatures. Besides, the refracted angle of each refracted beam in respective refracted plane can be set at will independently by changing the size of the supercell. Furthermore, since the supercell could be designed at a specific wavelength, the designed noncoplanar beam splitter can also function as a polarization-controlled dual-wavelength beam splitter. We believe such a noncoplanar beam splitter with tunable split ratio may play significant role in novel miniature optical devices and systems.

References

[1] Y. S. Kim *et al.*, "Informationally symmetrical Bell state preparation and measurement," *Opt. Express.*, vol. 26, no. 22, pp. 29539–29549, Oct. 2018.
[2] W. Wu, K. Zhou, C. Lu, and T. Xian, "Open-loop fiber-optic Gyroscope with a double sensitivity employing a polarization splitter and Faraday rotator mirror," *Opt. Lett.*, vol. 43, no. 23, pp. 5861–5864, Dec. 2018.
[3] J. Li *et al.*, "Efficient polarization beam splitter based on all-dielectric metasurface in visible region," *Nano. Res. Lett.*, vol. 14, no. 34, Jan. 2019, Art. no. 34.
[4] B. Wang *et al.*, "Rochon-prism-like planar circularly polarized beam splitters based on dielectric metasurfaces," *ACS Photon.*, vol. 5, no. 5, pp. 1660–1664, May 2018.

[5] M. Khorasaninejad and K. B. Crozier, "Silicon nanofin grating as a miniature chirality-distinguishing beam-splitter," *Nat. Commun.*, vol. 5, Nov. 2014, Art. no. 5386.
[6] F. Zhang, H. Yun, Y. Wang, Z. Lu, L. Chrostowski, and N. A. F. Jaeger, "Compact broadband polarization beam splitter using a symmetric directional coupler with sinusoidal bends," *Opt. Lett.*, vol. 42, no. 2, pp. 235–238, Jan. 2017.
[7] F. Zhang *et al.*, "On chip chirality-distinguishing beamsplitter," *Opt. Express*, vol. 25, no. 21, pp. 24861–24871, Oct. 2017.
[8] L. Chang, L. Liu, Y. Gong, M. Tan, Y. Yu, and Z. Li, "Polarization-independent directional coupler and polarization beam splitter based on asymmetric cross-slot waveguides," *Appl. Opt.*, vol. 57, no. 4, pp. 678–683, Feb. 2018.
[9] H. Qiu, J. Jiang, P. Yu, J. Yang, H. Yu, and X. Jiang, "Broad bandwidth and large fabrication tolerance polarization beam splitter based on multimode anti-symmetric Bragg sidewall gratings," *Opt. Lett.*, vol. 42, no. 19, pp. 3912–3915, Oct. 2017.
[10] Z. Wang, Y. Tang, L. Wosinski, and S. He, "Experimental demonstration of a high efficiency polarization splitter based on a one-dimensional grating with a Bragg reflector underneath," *IEEE Photon. Technol. Lett.*, vol. 22, no. 21, pp. 1568–1570, Nov. 2010.
[11] C. W. Berry, and M. Jarrahi, "Broadband terahertz polarizing beam splitter on a polymer substrate," *J. Infrared Millimeter Terahertz Waves*, vol. 33, no. 2, pp. 127–130, Feb. 2012.
[12] J. A. Grieve, K. F. Ng, M. J. L. F. Rodrigues, J. Viana-Gomes, and A. Ling, "Mechanically tunable integrated beam splitters on a flexible polymer platform," *Appl. Phys. Lett.*, vol. 111, no. 21, Nov. 2017, Art. no. 211106.
[13] A. V. Kildishev, A. Boltasseva, V. M. Shalaev, "Planar photonics with metasurfaces," *Science*, vol. 339, no. 6125, Mar. 2013, Art. no. 1232009.
[14] J. Chen *et al.*, "Enhancing the magnetic plasmon resonance of three-dimensional optical metamaterials via strong coupling for high-sensitivity sensing," *J. Lightw. Technol.*, vol. 36, no. 16, pp. 3481–3485, Aug. 2018.
[15] J. Chen *et al.*, "Engineering the magnetic plasmon resonances of metamaterials for high-quality sensing," *Opt. Express*, vol. 25, no. 4, pp. 3675–3681, Feb. 2017.
[16] J. Chen, H. Nie, T. Zha, P. Mao, C. Tang, X. Shen, and G. S. Park, "Optical magnetic field enhancement by strong coupling in metamaterials," *J. Lightw. Technol.*, vol. 36, no. 13, pp. 2791–2795, Jul. 2018.
[17] Z. Liu, X. Li, J. Yin, and Z. Hong, "Asymmetric all Silicon micro-antenna array for high angle beam bending in terahertz band," *IEEE Photon. J.*, vol. 11, no. 2, Apr. 2019, Art. no. 5900509.
[18] Z. Song, M. Wei, Z. Wang, G. Cai, Y. Liu, and Y. Zhou, "Terahertz absorber with reconfigurable bandwidth based on isotropic Vanadium Dioxide metasurfaces," *IEEE Photon. J.*, vol. 11, no. 2, Apr. 2019, Art. no. 4600607.
[19] J. Wang, J. Ma, Z. Hu, and X. Wu, "Terahertz metalens for multifocusing bidirectional arrangement in different dimensions," *IEEE Photon. J.*, vol. 11, no. 1, Feb. 2019, Art. no. 4600311.
[20] Y. Li *et al.*, "Orbital angular momentum multiplexing and demultiplexing by a single metasurface," *Adv. Opt. Mater.*, vol. 5, no. 2, Jan. 2017, Art. no. UNSP 1600502.
[21] H. Ren, X. Li, Q. Zhang, and M. Gu, "On-chip noninterference angular momentum multiplexing of broadband light," *Science*, vol. 352, no. 6287, pp. 805–809, May 2016.
[22] Z. Li, E. Palacios, S. Butun, and K. Aydin, "Visible-frequency metasurfaces for broadband anomalous reflection and high-efficiency spectrum splitting," *Nano Lett.*, vol. 15, no. 3, pp. 1615–1621, Mar. 2015.
[23] F. Aieta *et al.*, "Aberration-free ultrathin flat lenses and axicons at telecom wavelengths based on plasmonic metasurfaces," *Nano. Lett.*, vol. 12, no. 9, pp. 4932–4936, Aug. 2012.
[24] X. Ni, N. K. Emani, A. V. Kildishev, A. Boltasseva, and V. M. Shalaev, "Broadband light bending with plasmonic nanoantennas," *Science*, vol. 335, no. 6067 Jan. 2012, Art no. 427.
[25] Z. Guo, L. Zhu, F. Shen, H. Zhou, and R. Gao, "Dielectric metasurface based high-efficiency polarization splitters," *RSC. Adv.*, vol. 7, no. 17, pp. 9872–9879, Jan. 2017.
[26] A. Ozer, N. Yilmaz, H. Kocer, and H. Kurt, "Polarization-insensitive beam splitters using all-dielectric phase gradient metasurfaces at visible wavelengths," *Opt. Lett.*, vol. 43, no. 18, pp. 4350–4353, Sep. 2018.
[27] T. Kobayashi *et al.*, "Mach-Zehnder interferometer using frequency-domain beamsplitter," *Opt. Express*, vol. 25, no. 10, pp. 12052–12060, May 2017.
[28] T. Sun, P. Lu, Z. Zhuo, W. Zhang, and J. Lu, "Single-shot two-channel Fresnel bimirror interferometric microscopy for quantitative phase imaging of biological cell," *Opt. Commun.*, vol. 426, pp. 77–83, Nov. 2018.
[29] M. Wei *et al.*, "Broadband non-polarizing terahertz beam splitters with variable split ratio," *Appl. Phys. Lett.*, vol. 111, no. 7, Aug. 2017, Art. no. 071101.
[30] D. Zhang *et al.*, "Nanoscale beam splitters based on gradient metasurfaces," *Opt. Lett.*, vol. 43, no. 2, pp. 267–270, Jan. 2018.
[31] A. Arbabi, Y. Horie, M. Bagheri, and A. Faraon, "Dielectric metasurfaces for complete control of phase and polarization with subwavelength spatial resolution and high transmission," *Nat. Nanotechnol.*, vol. 10, no. 11, pp. 937–943, Nov. 2015.
[32] N. Yu *et al.*, "Light propagation with phase discontinuities: Generalized laws of reflection and refraction," *Science*, vol. 334, no. 6054, pp. 333–337, Oct. 2011.